Temperature dependence of positron trapping at grain boundaries

1997 J. Phys.: Condens. Matter 9 6749

(http://iopscience.iop.org/0953-8984/9/31/024)

J. Phys.: Condens. Matter **9** (1997) 6749–6759. Printed in the UK PII: S0953-8984(97)81290-8

Temperature dependence of positron trapping at grain boundaries

S Aina†, A Dupasquier†, P Folegati†, N De Diego‡, J del Rio‡, A Somoza§ and M Valli‖

† Dipartimento di Fisica, Politecnico di Milano, Piazza L da Vinci 32, I-20133 Milano, Italy
‡ Departamento de Física de Materiales, Facultad de Ciencias Físicas, Universidad Complutense, 28040 Madrid, Spain
§ IFIMAT, Universidad Nacional del Centro de la Provincia de Buenos Aires, Pinto 399, 7000 Tandil, Argentina
‖ ENEA, Centro Ricerche E Clementel, Via Don Fiammelli 2, I-40129 Bologna, Italy

Received 24 January 1997, in final form 16 April 1997

Abstract. Positron lifetime spectra were measured for fine-grained samples of the superplastic alloy Al–5 wt% Ca–5 wt% Zn at temperatures from 10 to 295 K. The lifetime attributed to annihilation from traps at the grain interfaces was found to increase with the temperature, while the corresponding intensity was observed to decrease. The quantitative analysis of the experimental results according to the diffusion-trapping model (Dupasquier *et al* 1993 *Phys. Rev.* B **48** 9235) leads to the following conclusions: (a) the positron diffusion coefficient in the alloy matrix (a solid solution of Zn and Ca in Al) is limited by positron–phonon scattering as well as by positron–impurity interaction; (b) the phonon-associated term in the reciprocal of the diffusion coefficient is dominant at room temperature and scales at other temperatures with the same power law as holds for pure Al (Soininen *et al* 1990 *Phys. Rev.* B **41** 6277); (c) the term associated with positron–impurity scattering is small except at very low temperatures, but the positron–impurity interaction seems to give a localization effect that is more important than the scattering; and (d) the specific trapping rate at the interface has a negative temperature dependence, as expected for trapping mediated by a precursor shallow state.

1. Introduction

Positron annihilation spectroscopy (PAS) is a well-established technique for the study of vacancies and small voids in solids, which gives quantitative information on defect structures, concentrations, and kinetics (for recent reviews see Hautojärvi and Corbel [1], Puska and Nieminen [2]). What makes positron spectroscopy very effective in this field of solid-state physics is not only the high sensitivity of the annihilation characteristics to the presence of defects, even at concentrations as low as a few parts per million, but also the possibility of interpreting the experimental data on the basis of simple and clear models that relate the observed quantities to defect concentrations and structures. The sensitivity of the positron annihilation method to extended defects (dislocations and internal surfaces) has also been known of for years, but the quantitative analysis of positron annihilation experiments is complicated in this case by the necessity of separating the effects related to the local structure of the defect from those arising from the geometry of the defect distribution. This requires one to take into account the spatial distribution of positrons at thermal equilibrium; to this end, the diffusion approximation is in principle adequate for

0953-8984/97/316749+11$19.50

most situations, but opens the way to an analytical approach only for highly symmetric geometries. Nevertheless, Dupasquier *et al* [3] and Pahl *et al* [4] showed recently that the essentials of the physical information can be brought out from the experimental data for real systems by using a model that includes in the correct way the main factors controlling the positron transport and trapping, in spite of the necessary simplification of the geometry. This point has recently been stressed by Dupasquier and Somoza [5] in a more general context.

In an application of the above ideas, we studied the temperature dependence of the positron trapping in the complicated 3D network of internal surfaces existing in a fine-grained Al-based alloy by measuring the positron lifetime spectrum at temperatures from 10 to 295 K and interpreting our results according to the diffusion-trapping model (DTM) developed in reference [3]. We obtain information regarding the temperature dependence of the positron diffusion coefficient D_+ and of the specific trapping rate at grain boundaries ν. The temperature dependence of the diffusion constant is a subject that has attracted considerable attention from the theoretical [6–12] as well as the experimental point of view [13–17]. Indeed, the knowledge of this dependence is a clue to much physics involving the state and the scattering mechanisms of the positron before trapping. The comparison of our results, which concern diffusion in the alloy matrix (a saturated solid solution of Ca and Zn in Al), with those obtained by Soininen *et al* [16] for pure Al is of interest as regards assessing the effect of substitutional impurities as scattering centres. The temperature dependence of the specific trapping rate at grain boundaries is also an interesting subject, as it opens the way to speculations on the structure of the grain boundary itself. The present work is the first exploration in this area. Information on the temperature dependence of specific trapping rates, for various defects other than grain boundaries, can be found in [2, 18–24].

2. Experimental procedure

The material chosen for this study is a commercial superplastic alloy (Al–5 wt% Ca–5 wt% Zn). The details of the thermal treatments adopted for obtaining different grain sizes are given in reference [3]. As shown by TEM images taken on samples in the conditions of the present experiment, the shape of the grains is approximately spherical, at least as far as is compatible with the condition of space filling. Two phases are present: (a) matrix grains (a solid solution of Ca and Zn in Al); and (b) a uniform distribution of spheroidized $CaZnAl_3$ particles (about 20 vol%). Choosing a bi-phase material may seem inappropriate in view of the applicability of a simple DTM for analysing the result of the experiment in terms of a small number of material parameters. However, this is a forced choice, since we need small grains for obtaining a measurable probability of positron trapping at internal surfaces, and second-phase particles nucleated as inter-grain precipitates are essential for blocking the growth of the matrix grains. On the other hand, reference [3] shows that the general trend of the annihilation parameters in different alloys at room temperature is essentially determined by the base metal and by the average grain size, without exhibiting much sensitivity to other details of the structure and of the composition. Therefore, we are encouraged to believe that the same model as was used in reference [3] can be applied to the present case.

We used three pairs of samples, with a selection of grain sizes convenient for enhancing the sensitivity of the lifetime spectrum to the positron diffusion constant (samples No 1 and No 2, with nominal domain radius $R = 1.4$ μm and $R = 0.9$ μm respectively) or, alternatively, to the specific trapping rate (sample No 3, with $R = 0.35$ μm). The domain radius is defined, according to reference [3], as the average radius of matrix grains

and second-phase particles ($CaAlZn_3$ inter-grain precipitates). In the present work, it was determined by the intercept method applied to optical or electronic micrographs.

Each pair of samples was assembled with a ^{22}Na source on 7.5 μm Kapton foils in the usual sandwich geometry. The source–sample sandwich was then mounted on the cold finger of a continuous-flow He cryostat. The temperature was monitored and automatically controlled within ± 1 K via a thermocouple in contact with the sample.

The lifetime spectrometer used for samples No 1 and No 2 (the 'ENEA' spectrometer) has a resolution of 205 ps (FWHM, full width at half-maximum of the prompt curve); it is based on Pilot-U scintillators, coupled to Philips XP2020/Q photomultipliers and commercial fast–fast ORTEC electronics. In order to avoid false prompt coincidences generated by two 511 keV γ-rays from the same annihilation event, the scintillator/photomultiplier assemblies were mounted with the axes crossing at 90°, and the source–sample sandwich was placed inside the cryostat cell at the crossing point of the axes. The spectrometer used for sample No 3 (the 'Madrid' spectrometer) has a FWHM of 225 ps; it is based on NE111 plastic scintillators coupled to Philips XP2020 photomultipliers plus commercial fast–fast ORTEC electronics. The scintillator/photomultiplier assemblies were mounted in the traditional 180° alignment, which has advantages in terms of geometrical efficiency; the same alignment was adopted for the measurements presented in reference [3]. In the case of complex lifetime spectra, the different mountings of the two set-ups may account for systematic lifetime differences of a few picoseconds, which are immaterial for our conclusions, which are mainly based on relative trends and parameters.

The number of coincidences in each spectrum was about 10^6. The analysis of the data was carried out by means of the POSITRONFIT computer program in the version contained in the PATFIT program package [25]. The main source component (12.5% at 382 ps) was subtracted separately, with an intensity fixed *a priori* in accordance with the results of Monge and del Rio [26]. Since we need at least three components to bring the variance of the fit (χ^2 per degree of freedom) close to 1 for the majority of the spectra, we adopted the three-terms scheme in all cases. The component with the longest lifetime, however, is just a tail with an intensity below 1% and a lifetime above 1000 ps, that we ascribe to residual source–surface effects. Discarding the tail, the significant part of the spectrum can be expressed in terms of the remaining two components, with the total intensity renormalized to 100%. According to the notation of reference [3], we label the intensities and lifetimes of the above components with the letters A and B in order of increasing lifetime.

The results are presented in figures 1 and 2. The data for the lifetime τ_B come from unconstrained fits; the intensity I_B and the lifetime τ_A were obtained by fixing τ_B at the value read from the linear regression line shown in figure 1. The statistical uncertainty is typically of the order of 5 ps for τ_A, 2 ps for τ_B, and 1% for I_B. The lines in figure 1 are linear or polynomial fits to the experimental data, and are drawn only as a guide to the eye. In contrast, the curves in figure 2 are the results of the DTM calculation, as discussed in the next section.

3. Interpretation

The decomposition of the lifetime spectra into components A and B, adopted here as well as in previous studies on positron trapping at grain boundaries, is a choice dictated by the limits of resolution and the statistics of the measurements, giving at least the advantage of producing data comparable with those from the other studies in this area. The disadvantage is that a decomposition scheme based on any finite number of exponential terms has only a limited physical meaning. We learn from the diffusion theory of positron trapping (see

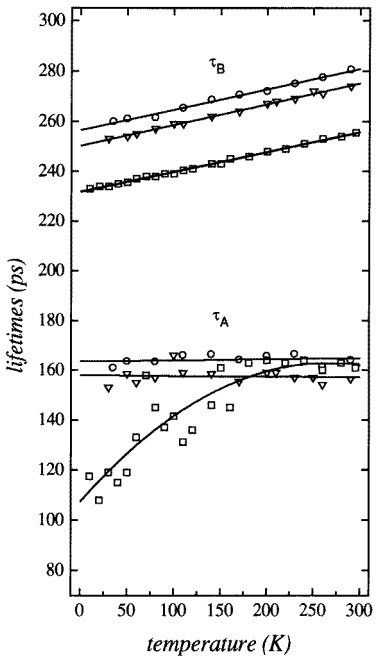

Figure 1. Lifetimes in fine-grained Al–Ca–Zn alloys versus the measurement temperature for three different grain sizes (circles: sample No 1, $R = 1.4$ μm; triangles: sample No 2, $R = 0.9$ μm; squares: sample No 3, $R = 0.35$ μm). The lines through the experimental points are first- or second-order regression polynomials, drawn as a guide to the eye.

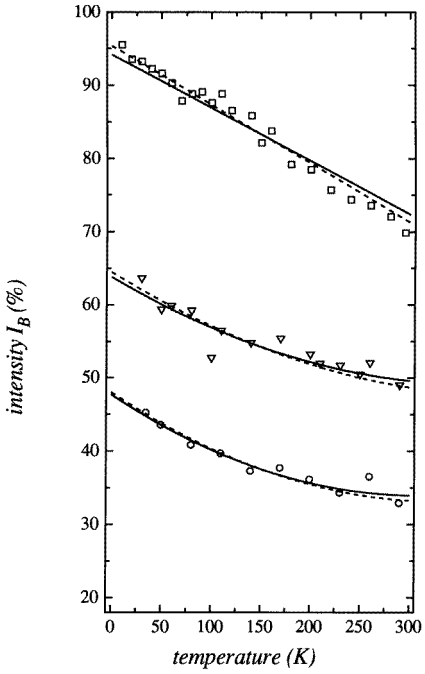

Figure 2. The intensity I_B versus the temperature. The symbols and samples are as for figure 1. Solid lines: DTM fits with $\delta_t = 500$ nm; broken lines: DTM fits with δ_t linearly decreasing with the temperature.

reference [3] and references therein; see also [27, 28]) that, when trapping is effectively limited by diffusion, the spectrum is formed by a slow exponential component, whose lifetime is a characteristic of the trapping surface, and a fast non-exponential component. The fast component can be represented as a series with an infinite number of exponential terms, with lifetimes shorter than the lifetime for the bulk material. Therefore, the two-terms fit is, strictly speaking, only a numerical approximation to the spectrum. In particular, the true mean lifetime τ_{fast} of the non-exponential part cannot come out from a best-fit procedure based on pure exponential decays. What actually happens is that the best-fit strategy gives more weight to the long-lifetime part of the fast component, which is less affected by the finite resolution of the apparatus, and contributes to the spectrum with more counts and for a longer time interval than the short-lifetime part. Thus the lifetime τ_A obtained from a two-terms POSITRONFIT analysis can only be longer than τ_{fast}. Qualitatively, we can associate τ_A with positrons thermalized far from a grain boundary. If the grains are big enough, these positrons have only a small probability of being trapped, and survive in the free state nearly as long as they would do in a bulk.

The above considerations allow us to explain the experimental behaviour of τ_A shown in figure 1 as follows. At high temperatures, τ_A remains very close to the bulk value for annihilation in Al, indicating that the positrons thermalized near to the centre of the grains are practically unaffected by the presence of a capturing surface at the grain boundary. This

means that the material contains a substantial fraction of grains with linear dimensions well above the positron diffusion length at these temperatures. At low temperatures, however, the diffusion length increases, and the situation may change. We actually see this effect for sample No 3, which is the sample with the smallest average size of the grains. In this case, not only does I_B rise to above 95% (see figure 2), but also τ_A falls below the bulk value. This description is consistent with the diffusion-trapping theory, but the ill-defined correspondence of τ_A with the theoretical mean lifetime τ_{fast} suggests that we should not go beyond the above qualitative description.

In spite of the inadequacy of a POSITRONFIT analysis for a spectrum containing a non-exponential component, the exponential part of the spectrum can be resolved correctly, if its lifetime is well separated from that of the bulk material. This condition is certainly fulfilled in the present case, as one can see by comparing the lifetime values τ_B reported in figure 1 (all above 230 ps) with the lifetime expected for a matrix of nearly pure Al (about 160 ps). Thus, we identify the slow exponential component predicted by the theory with component B obtained from the numerical analysis of the spectrum. In accordance with this identification, we interpret the lifetime τ_B as the reciprocal of the annihilation rate λ_{trap} of the positrons trapped at the grain boundaries. We also discuss below the quantitative interpretation of the I_B-data in terms of diffusion and trapping parameters in accordance with the DTM.

Figure 1 shows that the values of the long lifetime τ_B fall in a range typical of annihilation from trapped states in Al alloys; consistently with previous work on fine-grained systems (see reference [3] and references therein), we attribute this lifetime to annihilation from positron states localized at vacancy-like defects (open volumes) distributed over the grain interfaces. We observe small but distinct lifetime differences between the three samples, certainly related to a different morphology of the grain interfaces (a different distribution of open volumes). However, the increase of τ_B with the grain size, apparently suggested by the present data, is not to be taken as a true correlation, considering that no systematic grain size dependence was observed in reference [3], where the effect of the grain size on the annihilation parameters was specifically investigated for a large number of samples. Quite clear, in contrast, is a regular increase of τ_B with the temperature. Within the experimental accuracy, the temperature coefficient $((\mathrm{d}\tau_B/\tau_B)/\mathrm{d}T = (3.11 \pm 0.01) \times 10^{-4}\ \mathrm{K}^{-1})$ appears to be the same for the three pairs of samples. This coefficient is about four times the coefficient of thermal expansion of Al and of most Al alloys, which is of the order of $0.8 \times 10^{-4}\ \mathrm{K}^{-1}$. Temperature coefficients too strong to be related to the thermal expansion are not normally observed for the lifetime of positrons trapped at vacancy-like defects. Experimental evidence of strong temperature coefficients can, however, be obtained with extended defects (see, for instance, Bentzon *et al* [29]); the result has been interpreted as a combined effect of annihilation and transitions between states with lifetimes too close to be resolved independently. In the present case, the mechanism would be the following. The positron traps are open-volume sites of different dimensions. Small traps contribute to the average lifetime of the trapped positron with lifetimes shorter than the average, and big traps with lifetimes longer than the average. Since the binding energy of the positron is a decreasing function of the size of the trap, the small traps are shallower (less stable) than the big ones, and may be depopulated if the temperature is sufficiently high. Thus the weight of their contribution to the average lifetime of the ensemble of trapped positrons is a decreasing function of the temperature.

The temperature dependence of I_B displayed by the data of figure 2 implicitly reflects variations of transport and trapping factors, which can be made explicit with the help of the diffusion-trapping theory. This is what we plan to discuss here, after having recalled,

for the convenience of the reader, the basic assumptions and the main results of the DTM in the version presented in reference [3], where the mathematical details are given in full. The model assumes that the material is an aggregate of identical spheres *(domains)* with an effective radius R. The surface of each sphere is seen as a thin layer (thickness δ) where positrons can be trapped with a local trapping rate κ_s much larger than the annihilation rate inside the sphere (λ_{bulk}). The product $\nu = \kappa_s\delta$ is the trapping rate per unit specific surface (surface per unit volume); for brevity, we call ν the *specific trapping rate*. This is a material-dependent parameter that can be seen as a measure of the local disorder at the surface. The same physical information is expressed by the parameter $\delta_t = \delta\kappa_s/\lambda_{\text{bulk}} = \nu/\lambda_{\text{bulk}}$, hereafter called the *trapping thickness*, which we find more convenient to use in DTM calculations because of its dimensional homogeneity with the other two parameters (the domain radius and diffusion length) that control transport and trapping. The further assumption of the DTM is that the thermal positrons are created in each sphere with uniform probability, and migrate toward the surface as dictated by the diffusion equation, with allowance made for annihilation in the bulk. The positrons trapped at the surface are assumed to annihilate there with a characteristic annihilation rate λ_{trap}. De-trapping is not included in the model, but if no more than one component is resolved for the trapped positrons, the effects of de-trapping can be reabsorbed in a readjustment of λ_{trap} and of δ_t. The results of the theory presented in reference [3] can be summarized as follows.

(a) As already mentioned, the lifetime spectrum is formed by a slow exponential component, with lifetime $\tau_B = \lambda_{\text{trap}}^{-1}$ and a fast non-exponential component, represented as a series of decaying exponentials.

(b) The intensity I_B of the slow component is given by the sum of a series, which depends on three adimensional variables: the ratio ρ of the domain radius R to the diffusion length, $L_+ = \sqrt{D_+/\lambda_{\text{bulk}}}$, the ratio $\gamma = \lambda_{\text{trap}}/\lambda_{\text{bulk}}$, and the regime parameter $\alpha = \nu R/(\lambda_{\text{bulk}}L_+^2) = \delta_t R/L_2^+$.

(c) The general mathematical expression of I_B can be written in the form

$$I_B = 6\left(\frac{\alpha}{\rho}\right)^2 \sum_{n=1}^{\infty}[\beta_n^2 + \alpha(\alpha-1)]^{-1}[1-\gamma+(\beta_n/\rho)^2]^{-1} \tag{1}$$

where β_n is the nth solution of the eigenvalue equation

$$\beta_n \cot\beta_n + \alpha = 1. \tag{2}$$

(d) In the so-called transition-limited regime, corresponding to the limit $\alpha \to 0$, the series converges to the result of the standard trapping model (STM) with no allowance for diffusion, as given by the equation

$$I_B = \frac{\kappa}{\lambda_{\text{bulk}} + \kappa - \lambda_{\text{trap}}} \tag{3}$$

where κ is the product of the specific trapping rate ν and the surface per unit volume (specific surface $3/R$).

Our first step is the analysis of the data for the two samples with the largest grain size (samples No 1 and No 2). In this case (large regime parameter α), the analysis is simplified by the insensitivity of the DTM prediction for I_B to the trapping thickness δ_t, which enables us to ignore in a first approximation the possible temperature dependence of this parameter. This assumption will be modified later, on the basis of the results regarding the sample with the smallest grain size (sample No 3). For the moment, we assume, $\delta_t = 500$ nm which is the best-fit value assigned to this parameter in reference [3] on the basis of data taken at room temperature only. We then determine the best-fit values of the domain radius R for

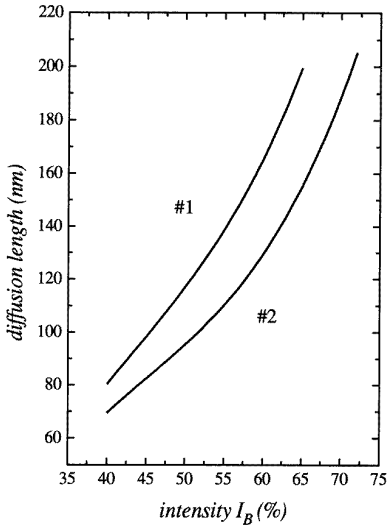

Figure 3. The diffusion length L_+ versus I_B for samples No 1 and No 2, as calculated from the DTM equations with $\delta_t = 500$ nm (see the text).

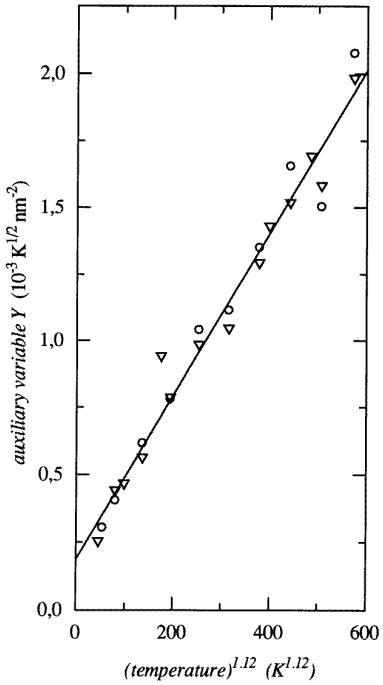

Figure 4. The auxiliary variable $Y = T^{1/2}/L_+^2$ versus $T^{1.12}$ for samples No 1 (circles) and No 2 (triangles). The straight line corresponds to the behaviour predicted by Blank *et al* [12].

samples No 1 and No 2 by requiring retrieval of the experimental value of I_B for samples No 1 and No 2 at room temperature (as read from the smoothed curves for I_B versus T) from the DTM calculation when not only δ_t but also the diffusion length is fixed at the value given in reference [3] ($L_+ = 95$ nm, corresponding to $D_+ = 0.55$ cm^2 s^{-1}). The best fit gives $R = 1.32$ μm for sample No 1 and $R = 0.82$ μm for sample No 2. These values include a 12% correction for taking into account the variability of the grain size in each sample (this point is discussed in reference [3]). The agreement with the intercept-method determination results (1.4 and 0.9 μm) is good, considering both the uncertainty of the experimental value (about 10%) and the geometrical simplicity of the model. After having determined R, we use again the DTM (equations (1) and (2)) for the numerical calculation of I_B as a function of L_+ for fixed values of δ_t and R. The result is shown in figure 3, where the two curves for L_+ versus I_B correspond to the R-values of samples No 1 and No 2. We use these curves for reading off the whole series of L_+-values corresponding to the I_B-points in figure 2. The result is presented in figure 4, as a plot of $Y = \sqrt{T}/L_+^2$ versus $T^{1.12}$; the reason for choosing this special representation will be discussed below. For the moment, we just note that the data points for both samples in figure 4 are well fitted by a single straight line. The calculation can now be repeated in reversed order for obtaining best-fit curves for I_B versus T according to the following steps: (a) starting from a temperature T, one finds the corresponding Y on the straight line in figure 4; (b) from Y and T, one calculates $L_+ = T^{1/4}/Y^{1/2}$; and (c) L_+ is used as an entry in the plots in figure 3, which leads to two values of I_B, one for each R. The results of the reversed calculation

are shown as solid lines for samples No 1 and No 2 in figure 2. The quality of the fits is good, but this is inherent to the calculation procedure and cannot be invoked to validate the model; the important point is that such good fits are obtained with a linear dependence of Y on $T^{1.12}$. Before proceeding any further it is convenient to comment on this result.

The choice of the special scales used in figure 4 is suggested by previous measurements and theoretical predictions regarding the temperature dependence of the positron diffusion coefficient in crystalline solids. The slow-positron beam experiments by Soininen *et al* [16] support a proportionality law $D_+ \propto T^{-0.62}$ for pure Al in the temperature interval from 16 to 505 K; this result is in agreement with the calculations of Blank *et al* [12] regarding positron scattering by acoustic phonons, with allowance made for the temperature dependence of the elastic constants (if this dependence is not included, one obtains the well-known, although incorrect, relationship $D_+ \propto T^{-1/2}$). Since the elastic constants of a diluted Al alloy change with the temperature in essentially the same way as for pure Al, we may expect, for the term depending on the phonon scattering ($D_{+,ph}$), the same scaling law, $D_{+,ph} \propto T^{-0.62}$. However, the effect of the positron–impurity scattering [9–12], that follows the different scaling law $D_{+,imp} \propto T^{1/2}$, cannot be neglected *a priori*. The combination of the two terms gives

$$D_+^{-1} = D_{+,ph}^{-1} + D_{+,imp}^{-1} \tag{4}$$

where the temperature dependence is expressed by the relationships

$$D_{+,ph}(T) = D_{+,ph}(300\ \mathrm{K})\left[\frac{300\ \mathrm{K}}{T}\right]^{0.62} \tag{5}$$

and

$$D_{+,imp}(T) = D_{+,imp}(300\ \mathrm{K})\left[\frac{T}{300\ \mathrm{K}}\right]^{1/2}. \tag{6}$$

Combining equation (4) with the definition of the auxiliary variable Y given above, one obtains

$$Y = AT^{1.12} + B \tag{7}$$

where

$$A = \frac{(300\ \mathrm{K})^{-0.62}}{D_{+,ph}(300\ \mathrm{K})\tau_{\mathrm{bulk}}} \tag{8}$$

and

$$B = \frac{(300\ K)^{1/2}}{D_{+,imp}(300\ \mathrm{K})\tau_{\mathrm{bulk}}}. \tag{9}$$

From the slope A and the intercept B of the straight line in figure 4, corresponding to equation (7), we estimate for $D_{+,ph}$ and $D_{+,imp}$ at room temperature the values 0.63 ± 0.02 cm^2 s^{-1} and 5 ± 1 cm^2 s^{-1}, respectively. Comparing the above results with the experimental value of the overall diffusion coefficient $D_+ = 0.55 \pm 0.05$ cm^2 s^{-1} (reference [3]), we find that the effect of positron–impurity scattering at room temperature is barely above the experimental errors, and cannot be invoked as explaining the difference between the positron diffusivity at room temperature for pure Al ($D_+ = 1.3$–2 cm^2 s^{-1}) [16] and for the Al matrix of the alloy. On the other hand, we find it hard to believe that a difference larger than 10 or 20% is the result of the imperfect adherence of the DTM to the real structure of our samples. We wonder whether we are not observing an impurity effect that cannot be described as a scattering mechanism. The concentration of Ca and Zn atoms dissolved

into the Al matrix is presumably of the order of 0.1 at.%. This is a small concentration, but still big enough to give more than four impurities in a volume comparable to the cube of the positron wavelength at room temperature. Thus the positron is not scattered by these impurities, but moves permanently in a disordered potential; for this reason, it has a tendency towards localization (see Nieminen [30]) that, in a diffusivity measurement, could be mistaken for a change in the parameters that characterize the Bloch states (the deformation potential E_d and effective mass m^*). Unfortunately, we are unable to evaluate whether the impurity concentration in our samples is sufficient to explain localization effects strong enough to cause a reduction of the diffusion coefficient by a factor of between 2 and 4.

The second part of our analysis relates to the interpretation of the I_B-data for the sample with the smallest grain size (sample No 3). As mentioned above, the reason for the separate treatment of these data is that the hypothesis of a temperature-independent capture thickness δ_t, justified in the analysis of samples No 1 and No 2 on the basis of the relative insensitivity of the DTM fitting to this parameter, may work less well in the case of a small domain radius. Nevertheless, we may proceed to a preliminary check of this hypothesis by fixing δ_t at 500 nm, as we have done before for samples No 1 and No 2. Since sample No 3 has the same composition and the same lattice as the other samples, we can also safely assume the same temperature dependence of $D_{+,ph}$. Most probably, the constant B (related to $D_{+,imp}$ by equation (9)) is also the same for all of our samples, but we prefer to keep B as a best-fit parameter together with the domain radius R. This choice may hide in part the effect of a change in δ_t, but guarantees that the origin of any deviation of the DTM model from the experimental data is not an incorrect assumption regarding B or R. Figure 2 shows that a small but real deviation does indeed exist. The DTM best fit with a fixed δ_t (the solid line, corresponding to $R = 0.4$ μm and $B = 0$) cuts through the sequence of the data points with a smaller slope than is needed to reproduce the observed temperature dependence (χ^2 per degree of freedom $= 2.5$). In order to improve the fit, the hypothesis of a temperature-independent value of the trapping thickness δ_t must be abandoned. For instance, choosing a decreasing linear dependence of δ_t from 600 nm at 10 K to 400 nm at 290 K gives the broken curve in figure 2 (χ^2 per degree of freedom $= 1.4$). The small systematic deviation that is still visible could certainly be cancelled with a more flexible assumption regarding the temperature dependence of δ_t, but playing with other adjustable parameters without the support of a theory would only be a mathematical exercise. The results mentioned above are already sufficient for telling us that the δ_t-variation occurring over the temperature range explored is negative, and amounts to at least 50% of the room temperature value. A stronger negative temperature dependence would have been obtained by taking for sample No 3 the same value of B as was used for samples No 1 and No 2.

As a final consistency check, we have recalculated I_B versus T for samples No 1 and No 2 with allowance made for the linear variation of δ_t mentioned above. The calculation shows that the new assumption regarding δ_t does not significantly affect the goodness of fit; indeed the new curves, reported in figure 2 as broken lines, are barely distinguishable from the solid lines obtained with a fixed δ_t. Therefore the conclusions drawn from the first part of the analysis can be taken as final.

4. Final remarks

We have observed a negative temperature dependence of the positron trapping at grain boundaries. A detailed analysis was made to correlate this effect with the temperature dependence of the positron diffusion coefficient and of the specific trapping rate. To this

end, we have adopted the diffusion-trapping model (DTM) developed in reference [3]. We have obtained the information summarized below.

4.1. The trapping thickness δ_t

This is a parameter, equivalent to the specific trapping rate $\nu = \delta_t \lambda_{bulk}$, that is related to the quantum rate of transition from the free state to the trapped state, and to the density of the trapping sites on the grain interface. It gives information on the surface structure complementary to that contained in τ_B, a parameter related to the dimensions of the open volume that is locally probed by the positron in the trapped state. Previous studies of trapping rates at internal surfaces are very few (see [5] and references therein), so the present investigation brings us onto almost unexplored ground. We have found an indication of a negative temperature dependence of δ_t, which is in contrast with experimental [31] and theoretical [32] evidence regarding trapping at surface states. However, the comparison with trapping at free surfaces is not meaningful, since we are facing here a hybrid situation where the inter-grain surface is seen as a continuum in the initial state (the positron in a Bloch state at thermal energies), but as a collection of independent trapping sites in the final state (the positron presumably localized in an open-space site of atomic or sub-atomic dimensions at the grain boundary). Negative temperature coefficients for specific trapping rates are found for positron trapping into kinks and jogs at dislocation lines in metals [21] and for trapping at negatively charged vacancy-like defects in semiconductors [33]. This behaviour is ascribed to a mechanism of mediated capture in the final trap via a weakly bounded precursor state. In the present case, one might think of small and large open-volume regions on the grain interface as respectively precursor and final traps. This hypothesis is consistent with the tentative explanation of the strong positive temperature coefficient of the lifetime τ_B that we proposed in the previous section.

4.2. The diffusion coefficient D_+

This is the crucial parameter governing positron transport from the point of thermalization to the trapping site. Our observations are consistent with a temperature dependence of the phonon-limited term $D_{+,ph}$ described by the $T^{-0.62}$-law already established for pure Al [16, 12]. We also find that the effect of positron–impurity scattering is weak at room temperature, in spite of the presence of substitutional impurities at concentrations near to saturation. Nevertheless, the value that we find for diffusion in the Al matrix of the alloy is two to four times smaller than accepted values for pure Al. We conjecture that the presence of substitutional impurities with a mean separation smaller than the positron thermal wavelength (i.e. in concentrations of the order of 0.1 at.% or greater) may affect $D_{+,ph}$ by giving an apparent modification of the effective mass and of the deformation potential of the positron. A positron beam experiment on a single crystal of Al with a well-known impurity content might give a conclusive answer on this important point.

References

[1] Hautojärvi P and Corbel C 1995 *Positron Spectroscopy of Solids* ed A Dupasquier and A P Mills Jr (Amsterdam: IOS Press) p 491
[2] Puska M J and Nieminen R M 1994 *Rev. Mod. Phys.* **66** 841
[3] Dupasquier A, Romero R and Somoza A 1993 *Phys. Rev.* B **48** 9235
[4] Pahl W, Gröger V, Krexner G and Dupasquier A 1995 *J. Phys.: Condens. Matter* **7** 5939
[5] Dupasquier A and Somoza A 1995 *Mater. Sci. Forum* **175–178** 35

[6] Seeger A 1972 *Phys. Lett.* **40A** 135
[7] Seeger A 1972 *Phys. Lett.* **41A** 267
[8] Seeger A 1973 *J. Phys. F: Met. Phys.* **3** 248
[9] Bergersen B and Pajanne E 1974 *Solid State Commun.* **15** 1377
[10] Bergersen B, Pajanne E, Kubica P, Stott M J and Hodges C H 1974 *Solid State Commun.* **15** 1377
[11] Boev O V, Puska M J and Nieminen R M 1987 *Phys. Rev.* B **36** 7786
[12] Blank R, Schimmele L and Seeger A 1992 *Mater. Sci. Forum* **105–110** 603
[13] Lynn K G and Lutz H 1980 *Phys. Rev.* B **22** 4143
[14] Schultz P J, Lynn K G and Nielsen B 1985 *Phys. Rev.* B **32** 1369
[15] Huomo H, Vehanen A, Bentzon M D and Hautojärvi P 1987 *Phys. Rev.* B **35** 8252
[16] Soininen E, Huomo H, Huttunen P A, Mäkinen J, Hautojärvi P and Vehanen A 1990 *Phys. Rev.* B **41** 6277
[17] Mäkinen J, Corbel C and Hautojärvi P 1991 *Phys. Rev.* B **43** 12 114
[18] Hodges C H 1970 *Phys. Rev. Lett.* **25** 284
[19] Hodges C H 1974 *J. Phys. F: Met. Phys.* **4** L230
[20] Bergersen B and McMullen T 1977 *Solid State Commun.* **24** 421
[21] Smedskjaer L C, Manninen M and Fluss M 1980 *J. Phys. F: Met. Phys.* **10** 2237
[22] Shirai Y and Takamura J 1989 *Mater. Sci.* **37** 123
[23] Jensen K O and Walker A B 1992 *J. Phys.: Condens. Matter* **4** 1973
[24] Trumpy G and Petersen K 1994 *J. Phys.: Condens. Matter* **6** 7843
[25] Kirkegaard P, Pedersen N J and Eldrup M 1989 *Patfit88: a Data-Processing System for Positron Annihilation Spectra on Mainframe and Personal Computers* (Roskilde: Risø National Laboratory Press)
[26] Monge M A and del Rio J 1994 *J. Phys.: Condens. Matter* **7** 2643
[27] Kögel M 1966 *Appl. Phys.* A **63** 227
[28] Würschum R and Seeger A 1996 *Phil. Mag.* A **73** 1489
[29] Bentzon M D, Linderoth S and Petersen K 1985 *Positron Annihilation* ed P C Jain, R M Singru and K P Gopinathan (Singapore: World Scientific) p 485
[30] Nieminen R M 1995 *Positron Spectroscopy of Solids* ed A Dupasquier and A P Mills Jr (Amsterdam: IOS Press) p 443
[31] Nieminen R M, Laakkonen J, Hautojärvi P and Vehanen A 1979 *Phys. Rev.* B **19** 1397
[32] Nieminen R M and Laakkonen J 1979 *Appl. Phys.* **20** 181
[33] Mäkinen J P, Hautojärvi P and Corbel C 1992 *J. Phys.: Condens. Matter* **4** 5137